C002

Exploiting the Airwave for Land CSEM Reservoir Monitoring

M. Wirianto* (Delft University of Technology), W.A. Mulder (Shell International E&P BV) & E.C. Slob (Delft University of Technology)

SUMMARY

Displacement of oil by saline water leads to time-lapse differences in CSEM measurements. Because the time-lapse effect may be weak and difficult to observe, acquisition optimization plays an important role. Applying a horizontal dipole source on the surface creates a source-induced airwave component. We studied the effect of the airwave on time-lapse land CSEM measurements of resistivity changes after oil production by running numerical simulations for several configurations. Our study shows that the source-induced airwave is the predominant component in increasing the amplitude of the time-lapse fields, the difference between the recorded EM data before and after oil production. Moreover, the lateral extent of the depleted part of the oil reservoir is much better defined when the airwave is present.

Introduction

The presence of the non-conducting air layer is a problem for the frequency domain controlled-source electromagnetic (CSEM) method when used on land. The interaction between the source-excited monochromatic EM fields and the air layer creates a source-induced airwave component that may dominate the EM field measurements, making the signal from the subsurface hard to distinguish. This gets worse for time-lapse measurements of resistivity changes in an oil reservoir caused by production, when saline water with low resistivity displaced highly resistive oil. In deep-water marine CSEM surveying, the airwave component will attenuated by the highly conductive water column, leaving only a small contribution to the EM fields measured by receivers on the seabottom. However, in shallow-water marine and land CSEM applications, the airwave component is significant.

Various techniques have been proposed to remove the airwave from the CSEM field measurements. In marine applications with receivers on the seabottom, the airwave effect is overcome by separating the recorded signals into upgoing and downgoing components (Amundsen et al., 2006; van den Berg et al., 2008). This approach exploits the fact that the receiver plane on the seabottom vertically separates the air-sea interface and the subsurface. Therefore, the airwave contribution will only appear in the downgoing components while the EM fields from the subsurface appear in the upgoing components. Another approach is to model the airwave in the water column and then subtract it from the measured data (Lu et al., 2005; Nordskag and Amundsen, 2007). In land applications, the field measurements are usually done in transient mode to avoid the airwave, employing an impulse excitation of the electromagnetic source (Strack, 1992; Wright et al., 2002). This approach exploits the fact that the source-induced airwave propagates in the air with the speed of light, so the airwave signal only appears at early times and can be removed easily by applying an appropriate filter. However, airwaves generated by EM fields that have gone down and returned to the surface will remain. Another approach is by applying two grounded dipole current sources that have dipole moments opposite to each other (Davydycheva et al., 2006).

Up till now, the airwave was considered as a signal that may not give any useful contributions, and should be removed from the measured data. Here, we present a modelling exercise to investigate the potential usefulness of the airwave in time-lapse land EM measurements for reservoir monitoring. We selected a simple half-space model and conducted numerical experiments to study the sensitivity of EM data to the changes in an oil-bearing reservoir due to water injection. Our results illustrate the positive contribution of the airwave towards detection of the lateral extent of the time-lapse resistivity changes.

Reservoir Monitoring

A potential application of the CSEM method is monitoring a hydrocarbon reservoir during production. Water flooding or steam injection for oil production creates a resistivity change that may be detectable by time-lapse EM measurements. The main problem is whether or not such a change is detectable, and if so, if EM can do better than time-lapse seismics. The latter requires a porosity greater than 30% to have a significant velocity difference between a water- and hydrocarbon-bearing reservoir. With EM, the resistivity difference between hydrocarbons-saturated rocks and saline-water-saturated rocks can be two or three orders of magnitude, making CSEM potentially more suitable if this difference can be detected in the presence of repeatability errors and noise.

Several authors have investigated the feasibility of CSEM monitoring (Black and Zhdanov, 2009; Lien and Mannseth, 2008; Orange et al., 2009; Wirianto et al., 2009). In those studies, the complexity of investigation varies from marine to land applications, from simple layered to complex geological background model, and from vertically piston-like to laterally reservoir flooding. Here, we consider the same application as Wirianto et al. (2009) but for a homogeneous half-space model. We assume that the CSEM measurements are available in the frequency domain.

To illustrate the concept of the CSEM method for reservoir monitoring, we begin with the survey layout sketched in Figure 1. A current source is employed to excite electromagnetic fields that penetrate through the background medium and illuminate the target, in our case the depleted zone (Figure 1a). This zone

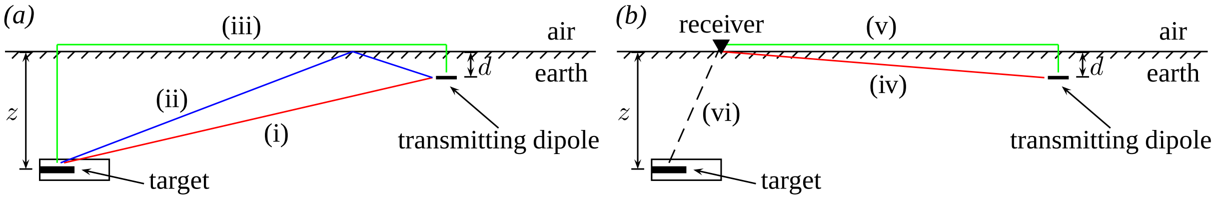

***Figure 1** (a) Path of EM fields at the depleted zone (target) from a HED source, consisting of the direct field* (i)*, the reflected field* (ii)*, and the airwave* (iii)*. (b) Path of EM fields at receivers, consisting of the direct field* (iv)*, the airwave* (v) *and the time-lapse field* (vi).

can be considered as a scatterer. The interaction between the excited EM signals and the scatterer results in a secondary field that can be detected with receivers on the surface in addition to the background field that would exist in absence of the depleted zone (Figure 1b).

The behaviour of the secondary fields is determined by the extent and the resistivity contrast of the depleted zone, as well as the background signals that are excited by the source. Since extent and resistivity contrast of the depleted zone are given, the detectability of the time-lapse change depends primarily on the background signals at the depleted zone. With a HED source, the background fields are generally composed of three type of fields: the direct incident field, the reflected field, and the airwave (Baños, 1966; King et al., 1992). The reflected field is due to the air-earth interface, which acts as a perfect reflector for some part of the field. When the HED source is placed on or close to the surface, the reflected field can be considered as the direct incident field. The background field is generally composed of the direct incident field and the airwave. Next, we investigate the effect of these fields on the detection of the depleted body.

Examples

Before considering a monitoring example, we examine the distribution of the current density for a point source in a half-space configuration. The current-density distribution excited by an x-directed HED point source in a homogeneous Earth model with a resistivity of 2 Ohm·m is presented in Figure 2. The source is located at (10,0,0) km, just below the air-earth interface, and operates at 1 Hz. The colour shows the magnitude of the current density, overlayed by the black arrows that point in the direction of the current-density vectors. The left panel shows the real part of the current density, while the right panel shows its imaginary part. At shallow depth, both the real and imaginary parts of the current density are decaying less in the lateral direction. This fact is due to the airwave.

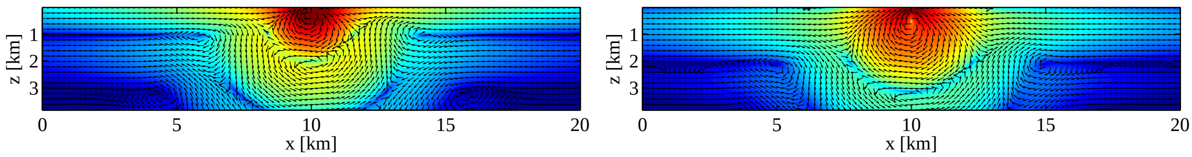

***Figure 2** Current-density vector plots for a 2 Ohm·m half-space model. All panels show the x, z-plane at y = 0 km. A harmonic x-directed point source is located at (10,0,0) km. The source frequency is set to 1 Hz. The background colour represents the amplitude of the current density on a logarithmic scale and the black arrows mark the directions of the current-density vectors. The top panel displays the real part of current density (the in-phase mode), whereas the bottom panel shows its imaginary part (the out-of-phase mode).*

Next, we include a reservoir under production. We take the same half-space model as before and insert a 300-m thick resistive hydrocarbon-bearing layer at 1 km depth with a resistivity of 100 Ohm·m and a 200-m thick conductive water-bearing layer with a resistivity of 3 Ohm·m. The top view of the reservoir is indicated in Figure 3. For the monitoring study, we assume the reservoir is flooded by saline water from the top left, creating a small, 100-m thick, box-shaped depleted zone in the corner of the hydrocarbon-bearing layer. The dashed line marks the water front of the flooded area. To observe the effect of the depleted zone, we consider the amplitude behaviour of the time-lapse difference for the in-line electric field, considering the amplitudes of the absolute differences as well as the normalized differences of the electric field. Figure 3 displays the amplitude behaviour of the time-lapse difference

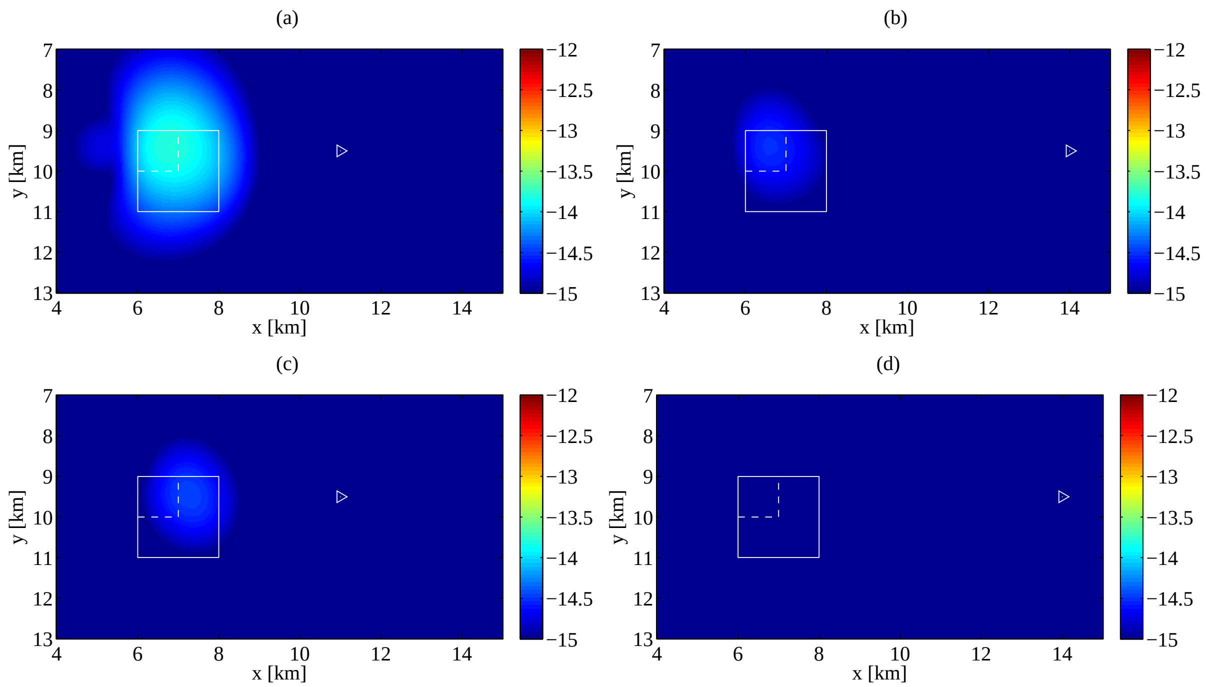

__Figure 3__ All panels shows $\log_{10}|\Delta E_1|$ at $z = 0$ km (top view). The top panels are with the homogeneous half-space background model, while the bottom panels are with the homogeneous full-space background model. The left panels are with a source at $(x, y) = (11, 9.5)$ km, while the right panels at $(x, y) = (14, 9.5)$ km. The solid white box indicates the lateral position of the reservoir and the dashed white line indicates the lateral position of the oil-water interface after flooding. The small white triangle marks the lateral location of the HED source.

for the in-line electric field, considering the amplitudes of the absolute differences. We considered four configurations, choosing from two background models and two source locations. The two background models are the homogeneous half-space and the homogeneous full-space model. The latter does not have an airwave. The two source positions are, respectively, at 3 and 6 km horizontal distance from the edge of the reservoir. Figure 2 shows that at 6 km distance away from the source the direct field is small and the airwave dominates. The top panels (3a and 3b) correspond to the homogeneous half-space background model and the bottom panels (3c and 3d) to the homogeneous full-space background model. The left panels (3a and 3c) have the source at 3 km and the right (3b and 3d) at 6 km distance. Comparing Figure 3a–b to Figure 3c–d, we observe that the airwave has a significant, positive contribution. The time-lapse difference signals are much stronger with the airwave present, even in the case of the source far away when the contribution of the direct incident field is small. Furthermore, the lateral extent of the depleted zone is much better defined with the airwave present. Unfortunately, if we assume a repeatability error of 1% in the time-lapse differences, these differences cannot be measured, as shown in Figure 4a–b. The cause is the airwave. As illustrated in Figure 1b, receivers also measure the airwave (the green line) besides the direct field (the red line) and the time-lapse field (the dashed line). To reduce the airwave effect at the receivers, we propose to run the same experiments but with a higher frequency, simultaneously. This proposal exploits the fact that the surface-to-surface CSEM method on high frequency has the same airwave effect but penetrates with shallow depth. Figure 4 shows the results. We computed the time-lapse difference field with the airwave subtracted by the result of frequency 10 Hz. Now, the lateral extent of the depleted zone is better defined, even in the presence of repeatability error.

Conclusions

With the HED source, the airwave appears as the predominant signal. The presence of the airwave is beneficial for the monitoring problem, because it provides illumination of the depleted zone even if the source is not close to the target. However, the strong currents induced by the airwave also dominate the time-lapse signals. This makes them difficult to detect in the presence of repeatability errors. To reduce

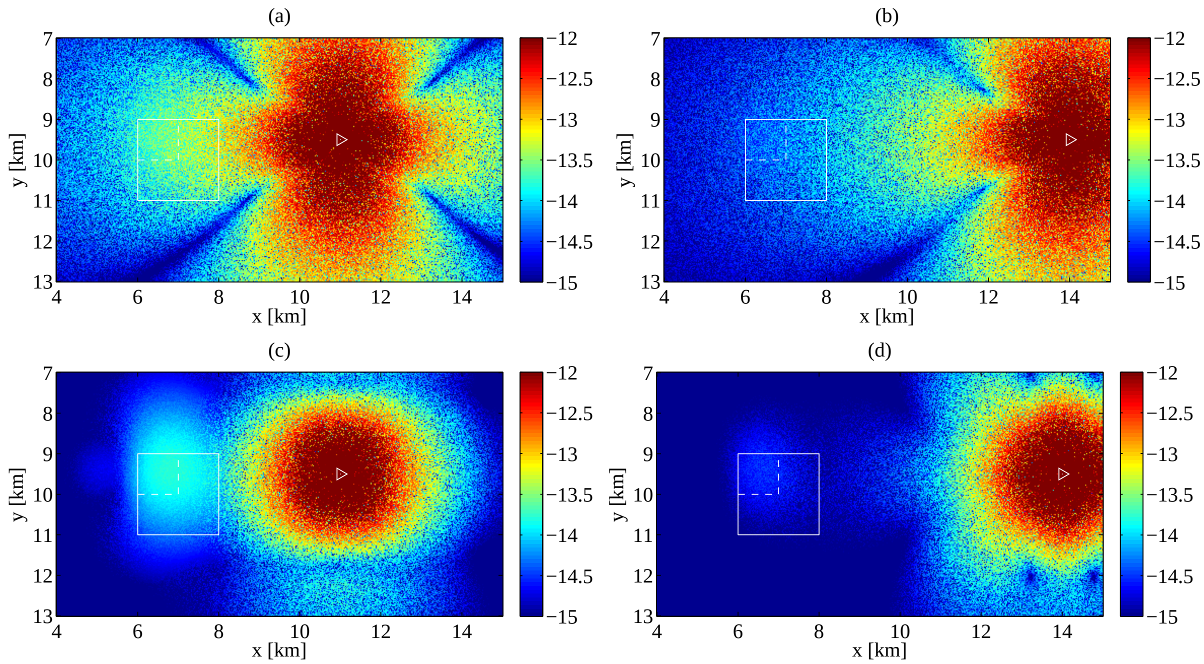

Figure 4 *The top panels show the same result as the top panels of Figure3, but with the presence of 1% repeatability error. The bottom panels shows the result after subtracting the response to the signals of 10 Hz.*

the airwave effect at the receivers, we propose to run the same experiment with a higher frequency, simultaneously. Our numerical results showed that the proposed method works fine. Nevertheless, we need to validate the method with some field experiments.

Acknowledgment

Marwan Wirianto received financial support from the sponsors of the Delphi consortium.

References

Amundsen, L., Løseth, L., Mittet, R., Ellingsrud, S. and Ursin, B. [2006] Decomposition of electromagnetic fields into upgoing and downgoing components. *Geophysics*, **71**(5), G211–G223.

Baños, A. [1966] *Dipole radiation in the presence of a conducting half-space*. Pergamon Press, Inc.

Black, N. and Zhdanov, M.S. [2009] Monitoring of hydrocarbon reservoirs using marine CSEM method. In: *79th Annual International Meeting SEG, Expanded Abstract*. Society of Exploration Geophysicists, 850–854.

Davydycheva, S., Rykhlinski, N. and Legeido, P. [2006] Electrical-propecting method for hydrocarbon search using the induced-polarization effect. *Geophysics*, **71**(4), G179–G189.

King, R.W., Owens, M. and Wu, T. [1992] *Lateral electromagnetic waves: Theory and applications to communications, geophysical exploration, and remote sensing*. Springer-Verlag New York, Inc.

Lien, M. and Mannseth, T. [2008] Sensitivity study of marine CSEM data for reservoir production monitoring. *Geophysics*, **73**(4), F151–F163.

Lu, X., Srnka, L.J. and Carazzone, J.J. [2005] Method for removing air wave effect from offshore frequency domain controlled-source electromagnetic data. *International patent application WO 2005/010560 A1*.

Nordskag, J.I. and Amundsen, L. [2007] Asymptotic airwave modeling for marine controlled-source electromagnetic surveying. *Geophysics*, **72**(6), F249–F255.

Orange, A., Key, K. and Constable, S. [2009] The feasibility of reservoir monitoring using time-lapse marine CSEM. *Geophysics*, **74**(2), F21–F29.

Strack, K.M. [1992] *Exploration with deep transient electromagnetic*. Elsevier.

van den Berg, P.M., Abubakar, A. and Habashy, T.M. [2008] Removal of sea-surface-related wavefields and source replacement in CSEM data processing. In: *78th Annual International Meeting SEG, Expanded Abstract*. Society of Exploration Geophysicists, 672–676.

Wirianto, M., Mulder, W.A. and Slob, E.C. [2009] A study of land CSEM reservoir monitoring in a complex 3D model. In: *71st EAGE Conference & Exhibition incorporating SPE EUROPEC 2009, Extended Abstract*. EAGE, X020.

Wright, D., Ziolkowski, A. and Hobbs, B. [2002] Hydrocarbon detection and monitoring with a multichannel transient electromagnetic (MTEM) survey. *The Leading Edge*, **21**, 852–864.